



# PREPARATION AND CHARACTERIZATION OF PHOTOCATALYTIC MODIFIED KAOLINITE CLAY CERAMIC MEMBRANE FILTER FOR REMEDIATION OF POLLUTED WATER



E. Ajenifuja<sup>1</sup>, J. A. Ajao<sup>1</sup> and E. O. B. Ajayi<sup>2</sup>

<sup>1</sup>Center for Energy Research and Development, Obafemi Awolowo University, Ile-Ife, Nigeria

<sup>2</sup>Department of Physics, Obafemi Awolowo University, Ile-Ife, Nigeria

<sup>3</sup>Department of Microbiology, Obafemi Awolowo University, Ile-Ife, Nigeria

\*Corresponding author: [eajenifuja@gmail.com](mailto:eajenifuja@gmail.com), [eajenifuja@cerd.gov.ng](mailto:eajenifuja@cerd.gov.ng)

Received: November 07, 2016

Accepted: March 05, 2017

**Abstract:** Photocatalytic ceramic membrane filter was prepared mainly from raw kaolinite clay. Ag-doped TiO<sub>2</sub> nanoparticles (STOX) were intercalated in the ceramic membrane to modify its properties. Characterizations of the materials were carried out using Fourier Transform Infrared (FTIR) Spectroscopy, Energy Dispersive X-ray Emission (EDX), Scanning Electron Microscopy (SEM) and X-ray Diffractometry (XRD). Ceramic membranes were formed by press method and subsequently subjected to a high temperature sintering treatment for physico-chemical stability. Ceramic membrane modules were constructed and experiments were carried out to test the remediation functionalities on polluted water using Atomic Absorption Spectrophotometry (AAS) and Total Bacterial Count Enumeration. Experimental results showed reduction in the concentration of Cd<sup>2+</sup>, Ni<sup>2+</sup> and K<sup>+</sup>, while increased concentrations were observed for Ca<sup>2+</sup>, Na<sup>+</sup> and Mg<sup>2+</sup>. Ceramic membranes exhibited highest flux output of 246.685 L/hr.m<sup>2</sup> under a transmembrane pressure of 0.0196 MPa. The antimicrobial microfiltration process indicated 100% bacterial removal and 70% fungi removal in most of the samples.

**Keywords:** Antimicrobial, ceramic membrane, photocatalysis, remediation, titanium dioxide

## Introduction

Clays play vital role in the environment by being a natural rummager of pollutants by taking on cation and anions through ion exchange and adsorption processes (Bhattacharyya and Gupta, 2008). Kaolinite clay is a ceramic raw material and finds applications in different technological products such as coatings, fillers, insecticide, medicine formulations, cosmetics, etc. The basic properties which mostly determines the use of the kaolinites for various applications, is its purity. Pure kaolinite (Al<sub>2</sub>O<sub>3</sub>·2SiO<sub>2</sub>·2H<sub>2</sub>O) is white in colour and its chemical composition is 46.54% SiO<sub>2</sub>, 39.50% Al<sub>2</sub>O<sub>3</sub> and 13.96% H<sub>2</sub>O (Grimshaw, 1971). However, presence of impurities, particularly iron- and titanium-bearing materials, causes colour to kaolin and reduces its refractoriness (Lee *et al.*, 2002; Ryu *et al.*, 1995). Therefore, mined kaolinitic aluminosilicate is usually associated with various impurities such as quartz, anatase, rutile, pyrite, siderite, feldspar, etc., depending on the origin and depositional environment (Grimshaw, 1971). These impurities impair the characteristics of kaolin and affect its utility for various end applications; nonetheless, the presence of impurity such as iron may have a positive influence on its utilization for water purification (Leiviskä *et al.*, 2012). The purification of raw clay is usually carried out by adopting various physical, chemical and biological processes as described in recent studies (Han *et al.*, 2003; Balachandran *et al.*, 2007; Ajenifuja *et al.*, 2012; Nickolov *et al.*, 2013; Ebrahimi *et al.*, 2012; Ebrahimi *et al.*, 2013; Lee and Cho, 2004; Lundquist *et al.*, 2006; Preston *et al.*, 1988; Clasen *et al.*, 2004; Ajenifuja *et al.*, 2016). In most cases, the aim is to dissolve some iron-bearing phases to lower the iron content of the clay.

Clay products are highly desired in environmental protection process, such as cleaning wastewater and filtering hot gas (Han *et al.*, 2003). Ceramic membranes from clay minerals have a wide range of domestic, industrial and scientific uses, the most common of which is the use in separation processes (Balachandran *et al.*, 2007; Ajenifuja *et al.*, 2012; Nickolov *et al.*, 2013). In term of durability, organic membranes are often used in industries and scientific establishments for separation and purification processes, but ceramic membranes offer

several advantages over organic membranes. Studies (Ebrahimi *et al.*, 2012; Ebrahimi *et al.*, 2013) have shown that ceramic membranes are more resistant than organic membranes to organic solvents, chlorine, and extremes of pH. Presently, ceramic separation membranes are being utilized in extreme conditions such as oil fields for separation of oilfield produced water. It is factual that ceramics are very resistant to severe chemical environments and are superior physically to the polymeric membrane, and as such they can be used for longer periods (Lee and Cho, 2004). Also, ceramic membranes are inherently more stable at high temperatures, thus allowing more efficient sterilization of process equipment than is possible with organic membranes.

In biological systems, ceramic membranes are generally quite resistant to microbial and biological degradation, which can occasionally be a problem with organic membranes. Recent studies (Lundquist *et al.*, 2006; Preston *et al.*, 1988; Ajenifuja *et al.*, 2012; Ajenifuja *et al.*, 2016) showed ceramic membranes to be efficient at retaining bacteria, virus and cysts through adsorption and depth filtration mechanisms. At domestic points of use, ceramic filters have been shown to reduce coliform bacteria resulting in greater than 70% reduction in cases of diarrhea (Clasen *et al.*, 2004). Despite that these ceramic membranes can trap bacteria; it has been shown that microbes can still grow on the media surface as biofilm (Lundquist *et al.*, 2006). Therefore, disinfection after filtration is usually necessary to control bacterial rejuvenation on the filtrate side of the membrane. Due to the problem of regeneration of pathogens on the surface of ceramic membranes; studies are being carried out for ways to hinder the regeneration. One way of combating surface biofilms formation is impregnation of membranes with antimicrobial agents such as silver nanoparticles.

Microbial and heavy metal pollutants removal studies using photocatalytically modified kaolinite clays are still relatively scarce, and there is still a need for more findings on the influence of mixed metal-oxide photocatalyst intercalation in kaolinite clay ceramic. Hence, efficiency of Ag-TiO<sub>2</sub> intercalated kaolinite clay ceramic was studied for degradation and removal of chemical and biological pollutants. In this work, thermally treated and mechanically

## The Preparation & Characterization of Photocatalytic Modified Kaolinite Clay

stable photocatalytic ceramic membranes were prepared from raw kaolinite clay and Ag-TiO<sub>2</sub> nanoparticles. Furthermore, pollutants degradation and removal tests were carried out to ascertain the potential of the ceramic membrane for water remediation.

### Materials and Methods

#### Raw materials

The kaolinite clay was collected from the exposed faces at a deposit site situated in Ijero Ekiti, Ekiti State, Nigeria. It is a soft, white clay mineral produced by the chemical weathering of aluminium silicate minerals like feldspar (Lee *et al.*, 2002; Grimshaw, 1971; Ryu *et al.*, 1995). The pure white colour of clay indicated that it contains little or no iron contamination which would have given it rusty colour (Grimshaw, 1971). The modifying materials are anatase TiO<sub>2</sub> nanoparticle (Hopkins & Williams) and AgNO<sub>3</sub>, which is the silver ion source. Sodium carbonate (99.0%, Na<sub>2</sub>CO<sub>3</sub>) was used to reduce the silver ions. The Ag-TiO<sub>2</sub> material expectedly served as a photocatalyst enhancing the remediation functionality of the main ceramic porous structure. Coir dust and carbon are examples of matrix biomaterials incorporated into the mesoporous ceramic membranes matrix.

#### Precursor preparations

The clay mineral was carefully separated from the rock matrix by gently crushing the portion of interest in a ceramic mortar. Therefore, a suspension of the pulverized material was prepared by adding the separated clay mineral particles to distilled water (1:5 clay to water ratio) in a 500 ml beaker; the kaolinite clay mineral totally immersed and soaked in the distilled water was left for about 2 h to aid dispersion of the clay particles in the water and for sol formation. Hence, the mixture was stirred for 20 min and left to settle for 2 min, enough for stone grains and other dense particles to coalesce at the bottom and maintaining the fine clay particles in suspension. The top milky sol was poured into a separate beaker. This process was repeated until a clear kaolinite clay mineral separate was obtained (Yoshihisa, 2001). The white clay paste was dried for 18 h at 100°C forming a soft cake. The physical and chemical properties of obtained kaolinite clay was beneficially enhanced using 30% dilute HNO<sub>3</sub>.

For the preparation of Ag-modified TiO<sub>2</sub> photocatalyst (STOX) (Wu and Chen, 2004; Sato *et al.*, 2005; Asahi *et al.*, 2001; Asahi and Morikawa, 2007; Zaleska, 2008). Firstly, 10 g of TiO<sub>2</sub> powder was placed into a 500 ml beaker with 100 ml ethanol as the dispersion medium. Then, 0.1M solution of AgNO<sub>3</sub> and 1% (w/v) solution of sodium carbonate (reducing agent) were prepared separately. To the dispersed TiO<sub>2</sub>, 4.6 ml of the prepared silver nitrate solution and 5 ml of sodium carbonate were added. The mixture was stirred vigorously for 2 h using a magnetic stirrer to form a slurry solution and afterwards the solid material (Ag-TiO<sub>2</sub>) was collected by centrifugation (Kondo and Jardim, 1991). The obtained Ag-TiO<sub>2</sub> was dried and calcined in the furnace at 100°C for about 24 h and at 400°C for 12 h, respectively in order to remove organic impurities and also induce thermal diffusion in the material.

#### Modified kaolinite clay ceramic preparation

Ag-TiO<sub>2</sub> intercalated kaolinite (STOX-K) was prepared from purified kaolinite powder (KLN) and Ag-TiO<sub>2</sub> colloidal solution (STOX). 25 g of KLN with about 2.5 g of coir dust was added slowly into the continuously stirred Ag-TiO<sub>2</sub> colloidal solution. The slurry formed was mildly heated for 2 h on the hot plate. The final modified kaolinite ceramic precursor was recovered from the slurry via sedimentation and filtration. Conspicuous visible light induced colour change was observed for the recovered modified kaolinite clay (STOX-K) particles when exposed to daylight (Page, 2009). The constituents of the ceramic precursors are highlighted in Table 1. Dead-end design configuration

was adopted for the casting of the ceramic membrane samples. The cast membrane samples KLN and STOX-K were sintered at temperature between 900 and 1000°C in the furnace for about 12 h for mechanical stability. The basic steps taken to prepare the ceramic membrane samples from the raw materials are illustrated in Fig. 1.

**Table 1: Constituents of the ceramic membrane precursor materials**

Sample	Constituents		
	Kaolinite clay	Ag-TiO <sub>2</sub> (Sol-Gel)	Coir
KLN	✓	-	✓
STOX-K	✓	✓	✓

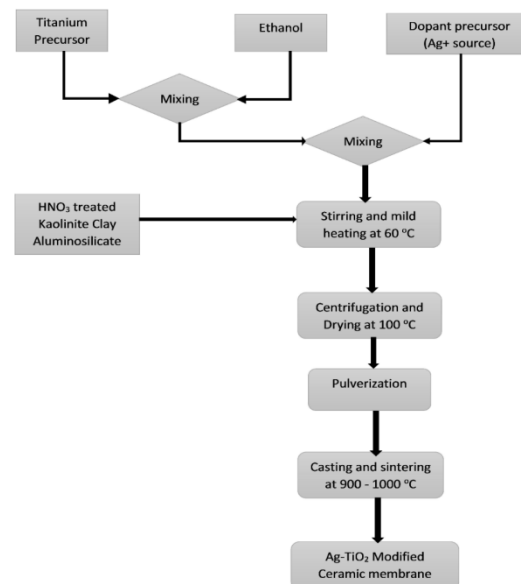


**Fig. 1:** Procedure of Ag-TiO<sub>2</sub> modified kaolinite clay ceramic membrane by thermal fusion

#### Chemical and thermal characterization methods

Energy dispersive X-ray (EDX) analysis was used for the elemental characterization, while chemical analysis of the materials was done using multi-functional Fourier Transform Infra-red (FTIR) spectrophotometer (Thermo Scientific NICOLET iS5) equipped with iD3 AIR sample holder at CERD. Differential Thermal Analyzer (DTA 404 PC *Éos*®) was used to study the thermal characteristics of the precursors. The morphologies of the natural and modified materials were examined using scanning electron microscopy (VEGA 3 TESCAN).

#### Functional characterization methods

Membrane functional studies on pollutants and microbes removal from contaminated water were done to ascertain the suitability of the prepared ceramic membrane samples for environmental remediation applications. Atomic Absorption Spectrometry (AAS) was used to analyze water samples obtained from remediation experiments. This analysis focused mainly on the concentrations of some beneficial elements such as calcium, potassium, sodium and magnesium, while other common heavy metal pollutants (cadmium and nickel) in contaminated water were also assessed. The microbiological analysis of the water samples was carried out using plate count method. The method relies largely on growth of bacteria colonies on a nutrient medium. The procedure involved making serial dilutions of the water samples in sterile water and were then cultivated on nutritional medium (agar) in dishes that were sealed and incubated. Typical media include agar for a general count or MacConkey agar for Gram-negative bacteria such as *E. coli*.

This approach is commonly used for the evaluation of the effectiveness of water treatment by the inactivation of representative microbial contaminants such as *E. coli* following ASTM D5465 (Hanaor and Sorrell, 2014; Hanaor *et al.*, 2011).

**Results and Discussions**

**Energy dispersive x-ray analysis**

The elemental constituents of the ceramic membrane materials were determined and the spectra obtained for the samples are shown in Figs. 2(a) and (b). Different peaks observed correspond to the elements present in the samples. The accuracy of EDX spectrum can be affected by various factors since many elements will have overlapping peaks (e.g., Ti  $K_{\beta}$  and V  $K_{\alpha}$ , Mn  $K_{\beta}$  and Fe  $K_{\alpha}$ ). From elemental compositions as shown in Table 2, both samples KLN and STOX-K contain slightly more aluminium than silicon. This was appropriate for the formulation of low-Si zeolitic materials with high cation exchange capacity because of presence of more replacement of  $Si^{4+}$  by  $Al^{3+}$  (Ajenifuja *et al.*,

2012). Expectedly, carbon and oxygen were detected in both samples as shown in the spectra (Fig. 2). However, Ti is only detected in the modified materials. No iron content was detected in the samples, corroborating the earlier assertion about the colour (white), which indicated an absence of iron in the raw material (Grimshaw, 1971; Lee *et al.*, 2002).

**Table 2: Elemental concentrations of kaolinite aluminosilicates using EDX technique**

Elements	Concentrations (wt. %)	
	KLN	STOX-K
C	6.22	5.93
O	57.27	51.61
Al	18.39	15.90
Si	17.99	15.80
Ca	-	1.16
Ti	-	9.33
Na	0.13	0.23
Fe	-	-

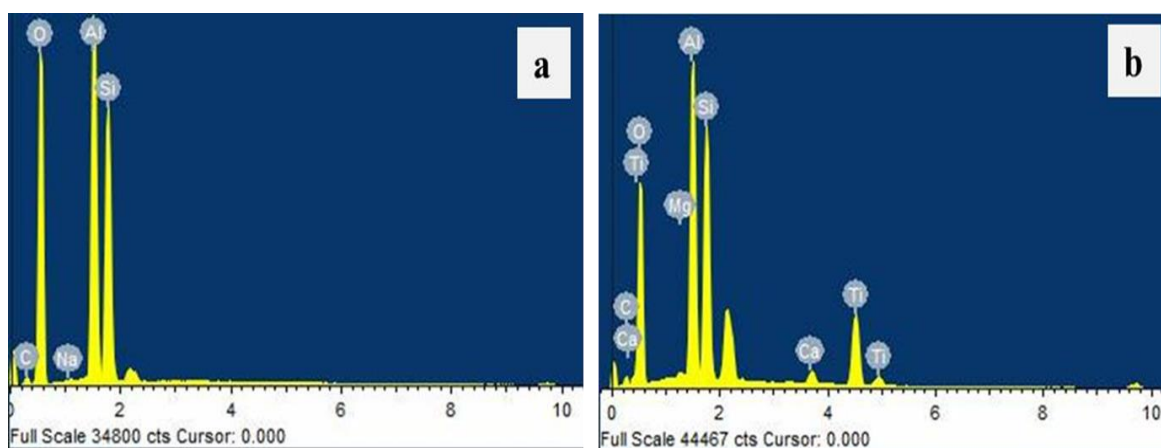


**Fig. 2: EDX spectra for samples (a) KLN, (b) STOX-K**

**Thermal properties of the raw and modified aluminosilicate materials**

The thermal behaviour of pure and Ag-modified  $TiO_2$  are shown together in Fig. 3. The thermal analysis was carried out to study the influence of heat on the physical and chemical properties of the kaolinite clay minerals. The curves obtained for the unmodified minerals are observed to show both exothermic and endothermic effects at temperature ranges peculiar to the behaviour of the minerals, thus showing the purity of the material. For instance, the pure and Ag-loaded  $TiO_2$  nanoparticles samples conspicuously exhibited an endothermic doublet peak at 798.4°C and 848.6°C (STOX) and 807.0°C and 858.1°C (TOX). The doublet endothermic peaks observed for the materials could be attributed to a successive decomposition and phase transitional recrystallization behaviour of the  $TiO_2$  nanoparticles. The lowering of the doublet endothermic temperature for sample STOX could be due to the influence of silver nanoparticles (Ag-NP) in the matrix. Studies (Greenwood and Earnshaw, 1984) have shown that metastable anatase and brookite  $TiO_2$  phases usually convert irreversibly to the equilibrium rutile phase upon heating above temperatures in the range 600°-800°C. Confirmed by the presence of the endothermic peaks, the pure and modified titanium oxide particles underwent drastic change in their crystal structures to form a rutile phase due to the application of heat. Slight left shifts in the successive peaks observed for sample STOX may not be

unconnected with presence of Ag-nanoparticles in the pure materials. A broad exothermic peak observed at 989.1°C for the modified sample STOX could be attributed to the Ag- $TiO_2$  nanoparticles solid state reaction encouraged by oxidation. This exothermic peak is not observed in the  $TiO_2$  thermal spectra.

The first peak observed for KLN in Fig. 4 is a low-temperature endothermic loop at 114.8°C closely followed by another set of endothermic peaks for both samples at 287.3 and 289.0°C. The first relatively low-temperature endothermic peak for KLN is usually registered when trapped atmospheric water molecules depart from the raw sample, while the second set of peaks observed for both samples is still part of the midrange temperature endothermic effect accompanying inner bound or molecular water, which obvious was not completely eliminated from the modified sample STOX-K despite the modification treatments. At the middle temperature range, deeper endothermic are observed for both materials between 500 and 600°C showing a common effect peculiar to clay/kaolinitic aluminosilicate materials and this is attributed to the dehydroxylation or the loss of OH groups in the aluminosilicate mineral structure. For typical kaolinite clay materials, endothermic dehydroxylation usually begins at 550 – 600°C to produce disordered metakaolin,  $[Al_2Si_2O_5(OH)_4 \rightarrow Al_2Si_2O_7 + 2H_2O]$ , but continuous hydroxyl loss (-OH) is observed up to 900°C and has been attributed to gradual oxidation of the metakaolin. A conspicuous endothermic

## The Preparation & Characterization of Photocatalytic Modified Kaolinite Clay

effect exhibited by STOX-K only, at 808.5°C indicates the presence of TiO<sub>2</sub> in the material structure. The endothermic effect between 726.5°C and 848°C has been shown to be the TiO<sub>2</sub> phase transformation temperature region. An onset of strong exothermic peaks is shown on the thermogram at about 1000°C for both samples which could be attributed to the solid state reaction of the TiO<sub>2</sub> material with main kaolinite clay mineral resulting in subsequent recrystallization and transformation of the already dehydrated material to mullite, cristoballite and quartz (Vaculikova and Plevova, 2005).

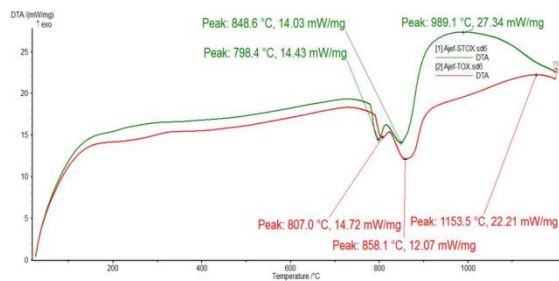


Fig. 3: DTA spectra for samples STOX and TOX

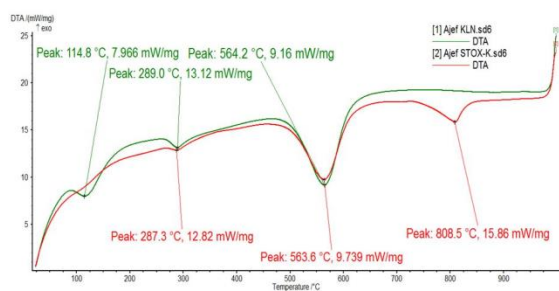


Fig. 4: DTA spectra for samples STOX-K and KLN

### FT-IR spectroscopy

FT-IR results for samples STOX-K and KLN are shown in Fig. 5. The spectra indicated a well crystalline kaolinitic nature with characteristic transmission bands at 3694 and 3626 cm<sup>-1</sup>

(Russell and Fraser, 1994; Balan, 2001) for the modified sample STOX-K, while similar bands are observed for the raw sample KLN at the same wave numbers. The observed bands are characteristic of kaolinite which arises from internal surface OH groups (OH<sup>-</sup> vibrations) or the possibility of hydroxyl linkage. The general feature of the OH stretching adsorption bands are well established for kaolin minerals (Farmer, 1974). A typical spectrum of kaolinite minerals usually shows four bands at 3697, 3669, 3645 and 3630 cm<sup>-1</sup> (Amorim *et al.*, 2004). The bands observed for the materials at 2916 and 2933 cm<sup>-1</sup> for STOX-K and KLN, respectively could be assigned to symmetrical stretch of C-H mode of -CH<sub>2</sub>- group. The OH deformation of water is found in between 1620-2642 cm<sup>-1</sup>. For the immediate range between 1620 and 1642 cm<sup>-1</sup>, the bending of water is observed. In the 1000 and 500 cm<sup>-1</sup> region, main functional groups were Si-O and Al-OH. For the samples, well resolved transmission bands are observed at 997, 993, 909 and 903 cm<sup>-1</sup> band which are within the range of the functional groups Si-O and Al-OH. The low transmission peaks exhibited from 799 to 680 cm<sup>-1</sup> on samples STOX-K and KLN are assigned OH deformation linked to Al<sup>3+</sup> and Mg<sup>2+</sup>. The bands 685 and 680 cm<sup>-1</sup> in STOX-K and KLN, respectively is very close to the band 693.4 cm<sup>-1</sup> assigned to Si-O and Si-O-Al stretching (Nayak and Singh, 2007). The main difference in the transmission bands to lower wavenumbers in sample STOX-K.

The IR results have been quite helpful in the identifications of various forms of minerals in the analyzed samples purportedly tested as adsorbents for heavy metals. Most importantly, the characteristic bands for kaolinitic aluminosilicate samples KLN and STOX-K at 3694 and 3626 cm<sup>-1</sup> have been shown to correspond, among others, basically H<sub>2</sub>O vibrations, indicating hydrous nature of the materials and presence of hydroxyl linkage. Also for the kaolinite samples is the presence of the high intensity broad doublet peak in the lower range of the transmission 700 – 1200 cm<sup>-1</sup> mostly corresponding to Si-O and Al-O stretching modes (Medioroz *et al.*, 1987).

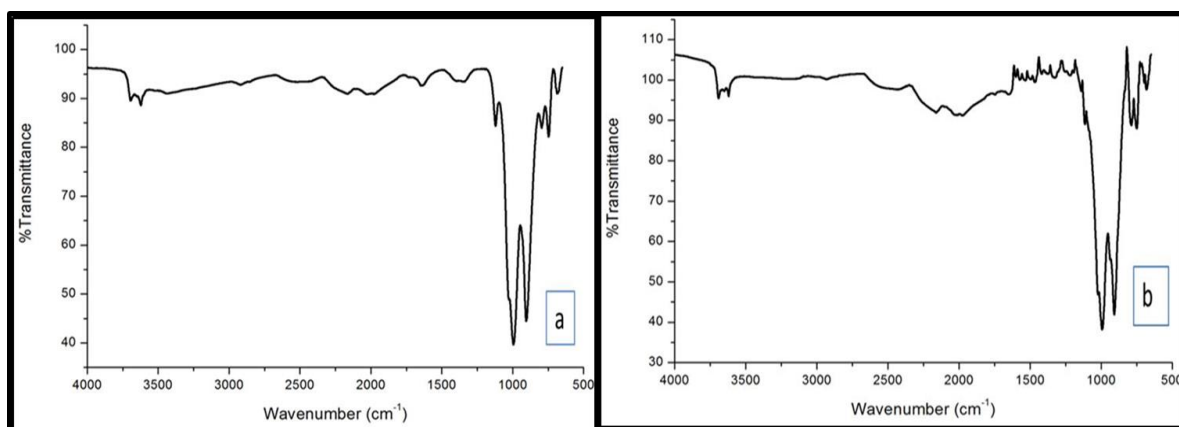


Fig. 5: FTIR spectra of (a) modified sample STOX-K, (b) unmodified sample KLN

### Surface microstructural analyses

The surface microstructure study of STOX-K and KLN was carried out using scanning electron microscope. The samples, being non-conductive were initially coated with an ultrathin

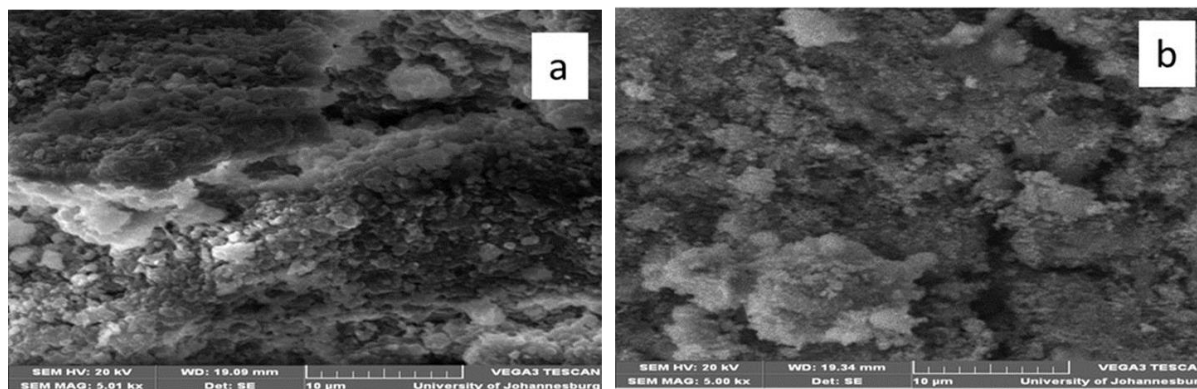
coating of electrically conducting material, deposited on the samples by low-vacuum sputter coating. The images acquired for the samples are shown in Fig. 6 (a, b). For modified kaolinite (STOX-K), the image showed well dispersed

## The Preparation & Characterization of Photocatalytic Modified Kaolinite Clay

particles and coagulates of the Ag-TiO<sub>2</sub> nanoparticles interspersed in the natural microstructure. The advantageous effect of the loaded TiO<sub>2</sub> nanoparticles in the structure would be by enhancing the fluid flow through the ceramic membrane; this is achieved by increment in the spacing between adjacent layers in the clay microstructure (Bhattacharyya and Gupta, 2008).

Furthermore, insertion of pore forming additives (coir) in the matrix would also contribute to the porosity. The photocatalytic nature of the Ag-TiO<sub>2</sub> would be much helpful in degrading both chemical and biological pollutants through the formation of hydroxyl radical on the catalyst surface (Asahi *et*

*al.*, 2001; Matsunaga *et al.*, 1985; Yin *et al.*, 2013; Akiyama *et al.*, 1998; Cowan *et al.*, 2003; Lansdown, 2006). The image for STOX-K membrane showed a distinct microstructure from that of KLN, which is possibly due to the chemical synthesis route that eliminated most of the impurities in the modified structure. STOX-K ceramic membrane is shown with well dispersed and distinct aggregates of particles, whereas, KLN ceramic membrane is shown to be constituted of closed packed globular microstructure. It is observed that for kaolinite-based ceramic membranes the flow channels are mostly located at the grain boundaries.



6: SEM micrographs for mesoporous ceramic membranes (a) KLN, (b) STOX-K

### Membranes functional physico-chemical studies

Analytical results from flame Atomic Absorption spectrometry of the water samples corresponding to different ceramic membranes are presented in Table 3. The water samples were obtained after experimental filtration process. Test was done for common dissolved elements which serve as indicator for water quality such as K<sup>+</sup>, Ca<sup>2+</sup>, Na<sup>+</sup>, and Mg<sup>2+</sup>. The samples were also tested for the heavy metal (Ni<sup>2+</sup> and Cd<sup>2+</sup>) concentrations. The concentrations in sample RAW corresponds to the dissolved metal species in the source water. It was observed that the concentrations of Mg<sup>2+</sup>, Na<sup>+</sup> and Ca<sup>2+</sup> ions increased considerably in water samples obtained from STOX-K. This is very important to the study because these cations are crucial in the determination of water quality in term of hardness. It indicated that the water hardness increased with passage through the membrane. However, considering the filtrate from membrane KLN, K<sup>+</sup>, Ca<sup>2+</sup>, and Mg<sup>2+</sup> ion concentrations reduced remarkably. Furthermore, for cations, especially K<sup>+</sup> and Na<sup>+</sup> where concentrations became higher with ceramic filtration. This can be inferred as selective ion exchange behaviour of aluminosilicate materials, where the substitution of Si<sup>4+</sup> by Al<sup>3+</sup> results in having extra negative charge on the frame, thereby creating traps for positive ions: H<sup>+</sup>, Na<sup>+</sup>, K<sup>+</sup>, Ca<sup>2+</sup>, Cu<sup>2+</sup> or Mg<sup>2+</sup> which could be released and dissolved into the stream. For heavy metals such as Ni and Cd, present in the raw water, the result showed that their concentration reduced considerably in filtrate samples from both membrane samples.

Table 3: Atomic absorption spectroscopy results of water samples

Element	Concentrations in Water Samples (ppm)		
	RAW	KLN	STOX-K
K	1.450	1.250	0.800
Ca	24.500	18.350	27.500

Na	6.400	7.450	7.750
Mg	5.000	4.850	12.350
Ni	0.023	0.058	0.012
Cd	0.019	0.019	0.009

### Membrane functional antimicrobial studies

Comparison of the water quality between raw water and filtered water carried out on the water samples is shown in Table 4. The results showed that, for most of the samples, 100% bacterial population can be removed by the ceramic membranes. Total bacterial concentration (TBC) comprised one or more of the pathogenic bacterium such as *Escherichia coli*, *Salmonellae*, *Staphylococcus*, *Pseudomonas*, etc. For most of the ceramic membranes, the results showed that there were 100% reductions in bacterial population as detected in different agar media used. In this study, four different agar media were used for the microbial analysis namely; NA, EMB, MAC and SDA. The first three media were for bacterial growth, while the SDA was prepared for fungi growth detection. Nutrient agar is a general purpose medium supporting growth of a wide range of non-fastidious organisms. For all sample plates, except the raw untreated water (designated as raw), No colony was detected on the agar plates. The "Levine's formulation", also called EMB, is a slightly selective stain for Gram-negative bacteria such *E-coli*, *Salmonella*, *Shigella*, etc. On the EMB agar plates for most of the samples, no bacterial colony was detected. However, 8 and 4 cfu/ml values were detected for the untreated and KLN membrane treated water samples, respectively. The MAC (MacConkey, 1905) agar, similar to EMB, can be used for the isolation and differentiation of Gram-negative enteric bacilli. The medium was used to differentiate strains of *Salmonella typhosa* from members of the coliform group. For the fungi detection in the samples, Sabouraud dextrose agar (Sandven and Lassen, 1999) was used to culture fungi in petri dishes. It has a low pH that inhibits the growth of most bacteria, and

also contains the antibiotic gentamicin to specifically inhibit the growth of Gram-negative bacteria. The unmodified ceramic membranes (KLN) exhibited higher fungus growth, while STOX-K due to the effect of the modification showed lower microbial population.

**Table 4: Microbial population analysis**

Sample codes	Water sample	Bacterial Count (cfu/ml) in Different Agar			Fungi
		NA	EMB	MAC	
Membrane					
KLN	WS1	0	4	5	2
STOX-K	WS2	0	0	0	1
(Raw)	WS3	16	8	6	3
(OAU)	WS4	0	0	0	2

**Flux Output Characteristics**

The relations for the hydrostatic pressure due to the liquid alone and flux output are given, respectively as:

$$P = \rho gh \text{ (1)}$$

$$v = V/St \text{ (2)}$$

**Where:**  $\rho$  is the liquid density,  $g$  is the gravitational acceleration,  $h$  corresponds to the height of the liquid relative to the membrane,  $V$  is the filtrate volume,  $S$  is the surface area of the membrane filter, and  $t$  is the time.

Using the relations (1) and (2), the transmembrane pressure was found to be 0.0196MPa and the output flux at about 30°C was found to 246.685 L/hr.m<sup>2</sup> for STOX-K, which is the highest value. As shown in Table 5, modified KLN-based mesoporous ceramic membrane (STOX-K) has the highest flux output, which is an indication of better performance compared to other membrane samples. The raw treated material KLN does not possess natural pore structure similar to those of zeolites and diatomites, the increase in flux is mainly due to the intercalation of TiO<sub>2</sub> nanoparticles in the clay structure which increased the spacing between adjacent layers and hence creates more flow channels within the grain boundaries. This is indicated from the flux values for the porous photocatalytic ceramic membrane STOX-K.

**Table 5: Output flux of the ceramic membranes**

Ceramic Membrane	Surface Area (m <sup>2</sup> )	Output Flux at Room Temperature (L/hr.m <sup>2</sup> )
KLN	3.243 * 10 <sup>-4</sup>	34.262
STOX-K	3.243 * 10 <sup>-4</sup>	246.685

**Conclusions**

Photocatalytic porous natural ceramic membranes have been prepared from abundantly available pure white kaolinite clay minerals using less complicated procedures with relatively low operating cost. The detail properties of the raw and the modified materials were obtained via the elemental, chemical, thermal and microstructural characterization techniques. Functional analyses of the membranes were carried out and the results indicated efficient remediation properties on polluted water. Modified membranes STOX-K showed adsorption capacity for K, Ni and Cd ions. Significantly, ceramic membranes exhibited high capacity of up to 100% efficiency in terms of bacterial and 70% fungi removal from water. Flux output capacity showed that modification enhances the porosity of the kaolinite material more than 100% compare to KLN.

**Acknowledgement**

The support of Department of Physics and Centre for Energy Research and Development, Obafemi Awolowo University, Ile-Ife, Nigeria is gratefully appreciated.

**References**

Ajenifuja E, Ajao JA, Alayande SO, Bakare MK, Taleatu BA & Ajayi EOB 2016. Synthesis and Characterization of Pure and Ag-TiO<sub>2</sub>-Modified Diatomaceous Aluminosilicate Ceramic Membranes for Water Remediation. *J. Water Resource & Protection*, 8: 594-607.

Ajenifuja E, Akinwunmi, OO, Bakare MK, Ajao JA, Adeniyi IF & Ajayi EOB 2012. Remediation of Polluted Water Using Natural Zeolitic Aluminosilicates/Lateritic Clay Ceramic Matrix Membrane. *ISRN Ceramics*:2012.

Akiyama H, Yamasake O, Kanzaki H, Tada J & Arata J 1998. Effects of sucrose and silver on Staphylococcus aureus biofilm. *J. Antimicrob. Chemothe.*, 42:629-634.

Ambikadevi VR & Gopalakrishna SJ1997. Iron stain removal by bleaching and leaching techniques. *10th Kerala Science*, pp. 445- 448.

Ambikadevi VR & Lalithambika M 2000. Effect of organic acids on ferric iron removal from iron-stained kaolinite. *Appl. Clay Sci.*, 16: 133-145.

Amorim LV, Gomes CM, Lira HD, Franca KB & Ferreira H C 2004. Bentonites from Boa Vista, Brazil: Physical, Mineralogy and Rheological Properties. *Materials Res.*, 7(4): 583-593.

Asahi R & Morikawa T 2007. Nitrogen complex species and its chemical nature in TiO<sub>2</sub> for visible-light sensitized photocatalysis. *Chem. Phys.*, 339: 57-63.

Asahi R, Morikawa T, Ohwaki T, Aoki K & Taga Y 2001. Visible-light photocatalysis in nitrogen-doped titanium. *Science*, 293: 269-271.

Balachandran U, Lee TH & Doris SE 2007. Hydrogen production by water dissociation using mixed conducting dense ceramic membranes. *Int. J. Hydrogen Energy*, 32: 451 - 456.

Balan E 2001. First-principles modelling of the infrared spectrum of kaolinite. *American Mineralogist*, 86: 1321-1330.

Bhattacharyya KG & Gupta SS 2008. Adsorption of a few heavy metals on natural and modified kaolinite and montmorillonite: A review. *Advances in Colloid & Interface Sci.*, 140: 114-131.

Borggaard OK 1979. Selective extraction of amorphous iron oxides by EDTA from a Danish sandy loam. *J. Soil Sci.*, 30: 727- 734.

Bruvold WH & Ongerth JH 1969. Taste quality of mineralized water. *J. Amer. Water Works Assoc.*, 61: 170.

Clasen TF, Brown J, Collin S, Suntura O & Cairncross S 2004. Reducing Diarrhea Through the Use of Household-based Ceramic Water Filters: A Randomized, Controlled Trial in Rural Bolivia. *Amer. J. Trop. Medicine & Hygiene*, 70(6): 651-657.

Conley RF & Lloyd MK 1970. Improvement of iron leaching in clays: optimizing processing parameters in sodium dithionate reduction. *Ind. Eng. Chem. Process Des. Dev.*, 9(4): 595- 601.

Cowan MM, Abshire KZ, Houk SL & Evans SM 2003. Antimicrobial efficacy of a silver-zeolite matrix coating on stainless steel. *J. Ind. Microbiol. Biotechnol.*, 30: 102-106.

de Mesquita LM, Rodrigues T & Gomes SS 1996. Bleaching of Brazilian kaolins using organic acids and fermented medium. *Miner. Eng.*, 9(9): 965-971.

Ebrahimi M, Kovacs Z, Schneider M, Mund P & Bolduan P 2012. Multistage filtration process for efficient treatment of oil-field produced water using ceramic membranes. *Desalin. Water Treat.*, 42(1-3): 17-23.

## The Preparation & Characterization of Photocatalytic Modified Kaolinite Clay

- Ebrahimi M, Schmitz O, Kerker S, Liebermann F & Czermak P 2013. Dynamic cross-flow filtration of oilfield produced water by rotating ceramic filter discs. *Desalination and Water Treatment*, 51(7-9): 1762-1768.
- Farhount N 1989. *Ph.D Thesis: Beneficiation of kaolins of islands of Milos*. Athens.: National Technical University
- Farmer VC 1974. The layer silicates. In: Farmer, V.C., Ed., *The Infrared Spectra of Minerals*, Mineralogical Society, London, pp. 331-363.
- Greenwood NN & Earnshaw A 1984. *Chemistry of the Elements*. Oxford: Pergamon Press.
- Grimshaw RW 1971. *Physics and Chemistry of Clay* (4th ed.). London: Ernest Benn.
- Groudev SN 1999. Biobeneficiation of mineral raw materials. *Miner. Metall. Process.*, 16(4): 19–28.
- Han YS, Li JB, Chi B & Wen ZH 2003. The effect of sintering temperature on porous silica composite strength. *J. Porous Materials*, 10: 41–45.
- Hanaor DA & Sorrell CC 2014. Sand supported mixed-phase TiO<sub>2</sub> photocatalysts for water decontamination applications. *Advanced Engineering Materials*, 16(2): 248–254.
- Hanaor D, Michelazzi M, Leonelli C & Sorrell C C 2011. The effects of firing conditions on the properties of electrophoretically deposited titanium dioxide films on graphite substrates. *J. Europ. Ceramic Soc.*, 31(15): 2877–2885.
- Komskaja M, Dolin A & Yatsunova S 1971. Enrichment of kaolin. *Otkryt. Izobret. Prom. Obraztsy Tovar. Znaki*, 48(5): 42–56.
- Kondo MM & Jardim WF 1991. Photodegradation of chloroform and urea using ag-loaded titanium dioxide as catalyst. *Water Res.*, 25: 823-827.
- Lansdown AB 2006. Silver in Healthcare: an Enigma and Pathological Fascination. *The Bulletin of The Royal College of Pathologists*, 133: 36-38.
- Lee EY, Cho KS & Wook R H 2002. Microbial refinement of kaolin by iron-reducing bacteria. *Appl. Clay Sci.*, 22: 47–53.
- Lee S & Cho J 2004. Comparison of ceramic and polymeric membranes for natural organic matter (NOM) removal. *Desalination*, 160: 223-232.
- Leiviskä T, Gehör S, Eijärvi E, Sarpola A & Tanskanen J 2012. Characteristics and potential applications of coarse clay fractions from Puolanka, Finland. *Cent. Eur. J. Eng.*, 2(2): 239-247.
- Lundquist A, Clarke S & Bettin W 2006. *Filtration in the Use of Individual Water Purification Devices*. 5158 Blackhawk Road, APG, MD, 21010: U.S. Army Center for Health Promotion and Preventive Medicine (USACHPPM).
- MacConkey A 1905. Lactose-fermenting bacteria in feces. *J. Hyg.*, 5: 333-379.
- Matsunaga T, Tomoda R, Nakajima T & Wake H 1985. Photoelectrochemical Sterilization of Microbial-Cells by Semiconductor Powders. *FEMS Microbiology Letters*, 29(1-2): 211-214.
- Medioroz S, Pajares JA, Brito I, Pesquera C, Gonzalez F & Blanco C 1987. *Langmuir*, 3: 676-681.
- Nayak PS & Singh BK 2007. Instrumental characterization of clay by XRF, XRD and FTIR. *Bull. Mater. Sci.*, 30(3): 235-238.
- Nickolov R, Spassova I, Velichkova N, Khristova N, Dimitrova V & Tzvetkova P 2013. Hybrid materials as catalyst support in NO reduction with CO. *Microporous and Mesoporous Materials*, 165: 193–199.
- Page K 2009. *Photocatalytic Thin Films: Their Characterizations and Antimicrobial Properties*. London: University College London.
- Presto DR, Vasudevan TV, Bitton G, Farrah SR & Morel J 1988. Novel Approach for Modifying Microporous Filters for Virus Concentration from Water. *Applied and Environmental Microbiology*, 54(6): 1325-1329.
- Russell JD & Fraser AR 1994. Clay Mineralogy: Spectroscopic and Chemical Determinative Methods. In M. J. Wilson, *Infrared methods* (pp. 11 –67). London: Chapman & Hall.
- Ryu HW, Cho KS, Chang YK, Kim SD & Mori T 1995. Refinement of low-grade clay by microbial removal of sulfur and iron compounds using *Thiobacillus ferrooxidans*. *J. Ferment. Bioeng.*, 80: 46–52.
- Sandven P & Lassen J 1999. Importance of selective media for recovery of yeasts from clinical specimens. *J. Clinical Microbio.*, 37(11): 3731–2.
- Sato S, Nakamura R & Abe S 2005. Visible Light sensitization of TiO<sub>2</sub> photocatalysts by wet method N doping. *Appl. Catal. A*, 284: 131-137.
- Shoumkov S, Dimitrov Z & Brakalov L 1987. High gradient magnetic treatment of kaolin. *Interceram*, 36(6): 26– 28.
- Vaculikova L & Plevova E 2005. Identification of clay minerals and micas in sedimentary rocks. *Acta Geodyn. Geomater.*, 2 (138): 167-175.
- Veglio F & Toro L 1994. Process development of kaolin bleaching using carbohydrates in acid media. *Int. J. Miner. Process*, 41: 239– 255.
- Veglio F, Passariello B, Toro L & Marabini AM 1996. Development of a bleaching process for a kaolin of industrial interest by oxalic, ascorbic and sulphuric acids: preliminary study using statistical methods of experimental design. *Ind. Eng. Chem. Res.*, 35: 1680–1687.
- Wu JC-S & Chen CH 2004. A visible-light response vanadium-doped titania nanocatalyst by sol-gel method. *J Photochem. Photobiol A*, 163: 509-515.
- Yin J, Yang Y, Hu Z & Deng B 2013. Attachment of silver nanoparticles (AgNPs) onto thin-film composite (TFC) membranes through covalent bonding to reduce membrane biofouling. *J. Membrane Sci.*, <http://dx.doi.org/10.1016/j.memsci.03.060>.
- Yoshihisa B 2001. Highly porous silicate ceramics prepared from saponite clay. *Mineral*, 3(1): 35-38.
- Zaleska A 2008. Characteristics of Doped-TiO<sub>2</sub> Photocatalysts. *Physicochem. Problems of Mineral Processing*, 42: 211-222.